Liver INTERNATIONAL
OFFICIAL JOURNAL OF THE INTERNATIONAL ASSOCIATION FOR THE STUDY OF THE LIVER

Liver International ISSN 1478-3223

BASIC STUDIES

Aflatoxin genotoxicity is associated with a defective DNA damage response bypassing p53 activation

Ozge Gursoy-Yuzugullu[1,2], Haluk Yuzugullu[1,2], Mustafa Yilmaz[2] and Mehmet Ozturk[1,2]

1 Centre de Recherche INSERM, Institut Albert Bonniot, Université Joseph Fourier U823, Grenoble, France
2 Department of Molecular Biology and Genetics, BilGen Genetics and Biotechnology Research Center, Bilkent University, Ankara, Turkey

Keywords
aflatoxin – checkpoint – DNA damage response – liver cancer – p53

Abbreviations
AFB1, aflatoxin B_1; DMSO, dimethyl sulphoxide; HCC, hepatocellular carcinoma.

Correspondence
Mehmet Ozturk, PhD, Centre de Recherche INSERM/UJF U823, Institut Albert Bonniot, Université Joseph Fourier U823, Grenoble, France
Tel: +33476549410
Fax: +33476549413
e-mail: ozturkm@ujf-grenoble.fr

Received 14 September 2010
Accepted 10 January 2011

DOI:10.1111/j.1478-3231.2011.02474.x

Abstract

Background: Hepatocellular carcinoma (HCC) is a leading cause of cancer deaths. Aflatoxins, which may play a causative role in 5–28% of HCCs worldwide, are activated in liver cells and induce principally G → T mutations, including the *TP53* codon 249(G → T) hotspot mutation. The DNA damage checkpoint response acts as an antitumour mechanism against genotoxic agents, but its role in aflatoxin-induced DNA damage is unknown. *Aim:* We studied the DNA damage checkpoint response of human cells to aflatoxin B1 (AFB1). *Methods and results:* The treatment of HepG2 hepatoma cells with mutation-inducing doses (3–5 μmol/l) of AFB1 induced DNA adducts, 8-hydroxyguanine lesions and DNA strand breaks that lasted several days. Persistent phospho-H2AX and 53BP1 foci were also detected, but cell growth was not affected. AFB1-exposed HepG2 cells formed phospho-H2AX and 53BP1 foci, but failed to phosphorylate both Chk1 and Chk2. Huh7 hepatoma and HCT116 colorectal cancer cell lines also exhibited a similarly incomplete checkpoint response. p53 phosphorylation also failed, and AFB1-exposed cells did not show p53-dependent G1 arrest or a sustained G2/M arrest. These observations contrasted sharply with the fully functional DNA damage response of cells to Adriamycin. Cotreatment of cells with AFB1 did not inhibit p53 and $p21^{Cip1}$ accumulation induced by Adriamycin. Thus, the deficient checkpoint response to AFB1 was not due to an inhibitory effect, but could be explained by an inefficient activation. *Conclusion:* Genotoxic doses of AFB1 induce an incomplete and inefficient checkpoint response in human cells. This defective response may contribute to the mutagenic and carcinogenic potencies of aflatoxins.

More than 600 000 people die each year from hepatocellular carcinoma (HCC), mostly (> 80%) in developing countries (1). Dietary exposure to aflatoxins and infection with the hepatitis B virus are the major risk factors for HCC, the most frequent liver cancer in these areas (2). According to a recent study, about 25 200–155 000 of global HCCs may be attributable to aflatoxin exposure. Most cases occur in sub-Saharan Africa, Southeast Asia and China, where populations suffer both from a high hepatitis B virus prevalence and largely uncontrolled aflatoxin exposure in food. Thus, aflatoxins may play a causative role in 5–28% of all global HCC cases (3).

Aflatoxins are potent liver toxins, lethal when consumed in large doses. Sublethal exposures can induce chronic toxicity, and low levels of chronic exposure can result in neoplasia, primarily HCC, in many animal species (4). Aflatoxin exposure in humans may occur at high or low levels, depending on the level of dietary *Aspergillus* contamination. Acute exposure to high levels leads to lethal aflatoxicosis associated with liver necrosis. Chronic exposure to low levels of aflatoxin is not lethal, but highly hepatocarcinogenic. Acute exposure to high levels of aflatoxins (> 20 μg/kg/day) with aflatoxicosis rarely occurs (5). In contrast, > 90% of people at a high risk for aflatoxin-caused HCC are exposed to very low doses (0.01–0.3 μg/kg/day), but the exposition is chronic (3, 5).

Aflatoxin B1 (AFB1), the major aflatoxin product, is metabolized mainly in the liver to AFB1-8,9-*exo*-epoxide and 8,9-*endo*-epoxide. The *exo*-epoxide form of AFB1 binds to DNA to form the predominant 8,9-dihydro-8-(*N*7-guanyl)-9-hydroxy AFB1 adduct, leading to a more stable imidozole ring-opened AFB1–formamidopyrimidine adduct (5). The pseudo-half-life for loss of 8,9-dihydro-8-(*N*7-guanyl)-9-hydroxy AFB1 is short, but AFB1–formamidopyrimidine adducts are stable, accumulate for several days and remain detectable for several weeks in rat liver (6, 7). The initial 8,9-dihydro-8-(*N*7-guanyl)-9-hydroxy AFB1 adduct and AFB1–formamidopyrimidine adduct, individually or collectively, represent the likely chemical precursors responsible for the genotoxic effects of AFB1 (8). In addition, common oxidative DNA damage, leading to 8-hydroxydeoxyguanosine lesions, was observed in rat hepatic DNA following exposure to AFB1 (4, 9). AFB1 induces mainly G:C to T:A transversions (4). We (10, 11) and others

(12) have identified a hotspot G → T mutation at codon 249 of the *TP53* gene (encoding the mutant p53ser249 protein) in HCC tissues in patients exposed to aflatoxins. Later studies demonstrated that this mutation was also detectable in non-tumour liver samples (13), as well as in the plasma of 6% of healthy individuals, 15% of cirrhotic patients and 40% of HCC patients living in aflatoxin-contaminated areas (14). Thus, the AFB1-specific G → T mutation of *TP53* is frequently present in people exposed to aflatoxins before any clinically detectable liver tumour. Taken together, these observations provide strong evidence that low levels of AFB1 are highly mutagenic in people chronically exposed to this hepatocarcinogenic agent.

Eukaryotic cells have developed a powerful DNA damage response system to protect their genome integrity. DNA damage induces several cellular responses that enable the cell either to eliminate the damage or to activate senescence and apoptosis processes. DNA damage checkpoint proteins play a central role in co-ordinating repair and cell cycle progression to prevent mutation. Several kinases, including ATM, ATR, Chk1 and Chk2, adaptor proteins such as 53BP1 and downstream cell cycle control proteins such as p53 and Cdc25, are involved in damage sensing and cell cycle control. DNA repair mechanisms include direct repair, base excision repair, nucleotide excision repair, double-strand break repair and cross-link repair (15, 16).

8,9-Dihydro-8-(*N*7-guanyl)-9-hydroxy AFB1 and AFB1–formamidopyrimidine adducts appear to be removed primarily by nucleotide excision repair in mammalian cells, but other repair systems have also been implicated in bacteria and yeast (8). The mechanisms of the DNA damage checkpoint response to AFB1 are poorly known. Here, we explored the DNA damage checkpoint response of wild-type p53 human cells to AFB1 exposure. Our findings indicate that the checkpoint response to genotoxic and mutagenic doses of AFB1 is incomplete. AFB1-exposed cells failed to activate p53 and did not undergo cell cycle arrest or apoptosis, despite the presence of DNA adducts and the accumulation of DNA strand breaks.

Material and methods

Cell lines

HepG2 and Huh7 cell lines were cultivated as described previously (10). HCT116 and HCT116–p53$^{-/-}$ cell lines (17), gifts from B. Vogelstein, were cultivated in McCoy's cell growth medium (Gibco) supplemented with 10% heat-inactivated fetal calf serum and 1% penicillin and streptomycin solution (Gibco).

Cell treatment

Aflatoxin B1 (Sigma, St Louis, MO, USA) was dissolved in dimethyl sulphoxide (DMSO, Carlo Erba, Milano, Italy). Adriamycin (Sigma) and hydroxyurea (Sigma) were dissolved in distilled water. Aliquots were stored at − 20 °C. Working dilutions were prepared fresh and added in a complete cell culture medium. DMSO ($< 10^{-3}$ v/v dilution) and distilled water were used for negative control experiments. AFB1 treatment was performed in the presence of the S9-activation system for all HCT116, HCT116–p53$^{-/-}$ and some HepG2 experiments for enzymatic activation into the AFB1-8,9-*exo*-epoxide form. The S9 activation system was prepared as described previously (18, 19), with minor changes. Briefly, the S9-activation mixture was prepared with 0.20 g/l S9 fraction from Sprague–Dawley rat liver (Xenotech, Lenexa, Kansas, USA), 10.5 mmol/l isocitric acid (Sigma) and 1.8 mmol/l β-nicotinamide adenine dinucleotide phosphate sodium salt hydrate (Sigma). This mixture was filtered (0.45 μm) and used at a 1:10 dilution in the cell culture medium.

Aflatoxin B1-DNA adduct and 8-hydroxy-deoxyguanosine immunoperoxidase assays

Aflatoxin B1-DNA adducts and 8-hydroxydeoxyguanosine lesions were detected by immunoperoxidase assays, as described previously (20), with minor changes. Briefly, cells were treated with AFB1 or DMSO on coverslips, washed with phosphate-buffered saline and then fixed in ice-cold methanol. AFB1-DNA adducts were detected using a monoclonal antibody (6A10) against an imidazole ring-opened persistent form of the major *N*7-guanine adduct of AFB1 (21). Before the immunoperoxidase assay of AFB1 adducts, cells were treated with a buffer containing 15 mmol/l Na_2CO_3 and 30 mmol/l $NaHCO_3$ (pH 9.6) for 2 h at room temperature. For the AFB1 adducts and 8-hydroxydeoxyguanosine lesions, cells were treated with RNAse (100 μg/ml) in Tris buffer (10 mmol/l Trizma Base, 1 mmol/l EDTA and 0.4 mol/l NaCl; pH 7.5) for 1 h at 37 °C. After washing with phosphate-buffered saline, proteinase K (10 μg/ml) treatment was carried out for 7 min at room temperature. After rinsing with phosphate-buffered saline, DNA was denatured with 2N HCl for 10 min and cells were neutralized by soaking coverslips in 50 mmol/l Tris base for 5 min. After blocking for 1 h, cells were incubated with mouse 6A10 (Santa Cruz, Trevigen, France) or mouse anti-8-hydroxydeoxyguanosine (Trevigen, France) monoclonal antibody overnight at 4 °C. Anti-mouse HRP-conjugated secondary antibodies (Invitrogen, Carlsbad, CA, USA) were used for 30 min for primary antibody detection. Cells were stained with diaminobenzidine solution (Dako, Carpinteria, CA, USA), counter-stained with haematoxylin (Sigma), mounted with 80% glycerol and observed under an Olympus light microscope.

Post-treatment cell survival – colony-forming ability assay

Cell survival was determined by assessing cell growth in 100 mm dishes after exposure to AFB1 or Adriamycin. HepG2 cells were seeded in six-well plates and semiconfluent cells were exposed to AFB1 (0–50 μmol/l) in the presence of the S9-activation system for 4 and 24 h respectively. Control cells were exposed to Adriamycin

(0–5 μmol/l) in parallel experiments. Following exposure, 10^4 cells were seeded into 100 mm dishes. After 10 days of cell culture, colonies were fixed in cold methanol, stained with Crystal Violet (Sigma) and counted in triplicate experiments. Cell survival was calculated as the percent ratio of cell numbers in treated vs untreated cells. Survival parameters were determined by plotting survival data on a semi-log plot.

Western immunoblotting

These experiments were carried out as described previously (22). Proteins were subjected to electrophoresis using 10% or 4–12% Bis-Tris NuPAGE Novex Mini gel systems (Invitrogen), according to the manufacturer's instructions. For the detection of phosphorylated proteins, cell lysates were prepared according to the protocol provided by the supplier using the following lysis buffer: 20 mmol/l Tris (pH 7.5), 150 mmol/l NaCl, 1 mmol/l EDTA, 1 mmol/l EGTA, 1% Triton X-100, 1 mmol/l Na_3VO_4, 1 μg/ml leupeptin and 1 mmol/l phenylmethylsulphonyl fluoride. Following electrophoresis, proteins were transferred onto nitrocellulose membranes and analysed using antibodies against cleaved caspase-3 (Cell Signaling, Danvers, MA, USA), total p53 (Santa Cruz), $p21^{Cip1}$ (Calbiochem, Darmstadt, Germany), phospho-H2AX (Millipore, Billerica, MA, USA), phospho-Chk2, phospho-p53ser15, phospho-p53ser20 (all from Cell Signaling) and Calnexin (Sigma).

Senescence-associated β-galactosidase assay

Senescence-associated β-galactosidase activity was detected as described previously (22), using a senescent cell staining kit (Sigma).

Single-cell gel electrophoresis (comet) assay

Single- and double-strand DNA breaks were detected using alkaline and neutral comet assays respectively (23, 24). The alkaline comet was performed exactly as described (23). The neutral comet assay was conducted as described (24), using the lysis protocol described by Chandna (25). Following electrophoresis, slides were rinsed, stained with 5 μg/ml 4′,6-diamidino-2-phenylindole (Roche, Mannheim, Germany) and analysed under an Apotome (Zeiss, Germany) microscope. Images were captured with an Axiocam HRc colour CCD camera (Zeiss) and digitally saved using AXIO VISION software (Zeiss). Data were analysed by CASP (Comet Assay Software Project), which measures tail moment, using the DNA content in the tail and head along with the distance between the means of the head and tail distributions (http://casplab.com). At least 30 nuclei were analysed for each experimental condition.

Indirect immunofluorescence

Cells were fixed with 4% formaldehyde and permeabilized with phosphate-buffered saline supplemented with 0.5% saponine (Sigma) and 0.3% Triton X-100 (Sigma). After blocking for 1 h, cells were incubated overnight at 4 °C, with antibodies against Ser139-phosphorylated H2AX (phospho-H2AX; Millipore) or against 53BP1 (Abcam, Paris, France). After incubation with Alexa 568-conjugated secondary antibodies (Invitrogen), cells were counterstained with 4′,6-diamidino-2-phenylindole (Roche) and observed using an Apotome (Zeiss) microscope. Images were captured with an Axiocam HRc colour CCD camera (Zeiss) and digitally saved using AXIO VISION software (Zeiss).

Cell cycle analysis and bromodeoxyuridine incorporation assay

Cells were washed twice in phosphate-buffered saline and fixed in ice-cold ethanol for 10 min. After two phosphate-buffered saline washes, cells were incubated with 20 μg/ml of RNase A (Fermentas, Leon-Rot, Germany) at 37 °C for 10 min and stained with propidium iodide (10 μg/ml; Sigma). Cell cycle distribution was determined by flow cytometry using FACSCAN and CELLQUEST software (Becton Dickinson, Franklin Lakes, NJ, USA). Cell cycle analysis combined with the bromodeoxyuridine incorporation assay was performed using cells first labelled with 10 μmol/l bromodeoxyuridine (Sigma) for 2 h before each testing time. Cells were incubated with FITC-conjugated antibromodeoxyuridine antibody (BD Bioscience, Franklin Lakes, NJ, USA) at room temperature in the dark, following DNA denaturation with 4N HCl for 30 min (26).

Results

Induction of DNA adducts, 8-hydroxydeoxyguanosine lesions and DNA breaks by aflatoxin B1 in HepG2 cells

The human hepatoma line HepG2 has retained the activities of various phase I and phase II enzymes that play a crucial role in the activation and detoxification of genotoxic procarcinogens. It has been used successfully for genotoxicity assays for various classes of environmental carcinogens including aflatoxins, nitrosamines, aromatic and heterocyclic amines and polycyclic aromatic hydrocarbons, as well as for antimutagenicity studies (27). Furthermore, HepG2 has retained the wild-type activity of the p53 gene, a well-established DNA damage response gene (28, 29). Therefore, we first used the HepG2 cell line to test the genotoxic effects of AFB1. Cells were treated with 3–5 μmol/l of AFB1 in the absence or the presence of the S9-activating system that allows the activation of AFB1 into AFB1-8,9 epoxide (18). Following 24 h of exposure, cells were subjected to immmunoperoxidase assays to detect the imidazole ring-opened persistent form of the major *N*7-guanine adduct of AFB1 and 8-hydroxydeoxyguanosine DNA lesions. Our results verified the detection of AFB1 adducts in the nuclei of most cells with 3 or 5 μmol/l AFB1 (Fig. S1A). Adduct detection levels were quite similar between these two doses, indicating that AFB1 was capable of inducing highly abundant DNA adducts when tested at micromolar levels. We also observed the detection of

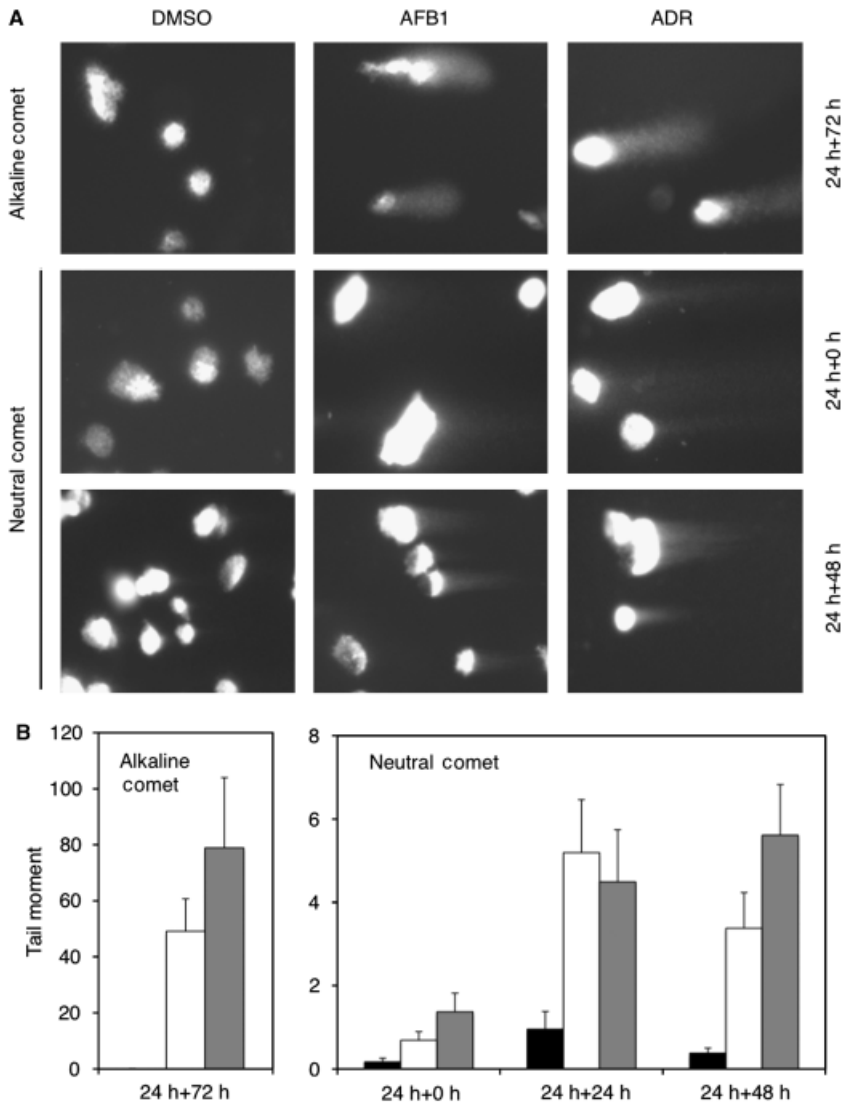

Fig. 1. Induction of persistent single- and double-strand DNA breaks in HepG2 cells following AFB1 exposure. (A) HepG2 cells were exposed to DMSO, AFB1 (5 μmol/l) or Adriamycin (0.5–1 μmol/l) as a positive control for 24 h, followed by a culture in the absence of test chemicals for up to 72 h, and subjected to alkaline comet or neutral comet assays to detect single- and double-strand breaks respectively. (B) Quantitative analysis of AFB1-induced DNA breaks by automated tail moment measurement. Black, white and grey columns indicate cells exposed to DMSO, AFB1 and Adriamycin respectively. Error bars indicate SD. AFB1- and Adriamycin-treated cells displayed significantly increased tail moments at all time-points tested ($P < 0.0001$). AFB1, aflatoxin B1; DMSO, dimethyl sulphoxide; SD, standard deviation.

8-hydroxydeoxyguanosine-positive nuclear foci (Fig. S1B). The same results were obtained in the presence or in the absence of the S9-activating system (Fig. S1).

The genotoxic effects of AFB1 were studied by alkaline and neutral comet assays that detect single- and double-strand DNA breaks respectively (23, 24). Examples of comet assay results are shown in Figure 1A. Both AFB1- and Adriamycin-exposed cells, tested by an alkaline comet assay at 72 h post-exposure time, displayed a statistically significant increase in comet tail moments ($P < 0.0001$), indicating the presence of abundant single-strand DNA breaks (Fig. 1B, left). A neutral comet assay also detected a statistically significant ($P < 0.0001$) increase in tail moments with both chemicals that lasted at least 48 h after the removal of chemicals from the cell culture medium (Fig. 1B, right). Tail moments obtained with the neutral comet were nearly 10-fold fewer than those obtained with the alkaline comet (Fig. 1B). Thus, AFB1 induced many more single-strand breaks than double-strand breaks.

Lack of significant growth inhibition in response to aflatoxin B1 exposure

Next, we studied the cellular response to AFB1-induced genotoxicity using cell growth, senescence and apoptosis

Liver International (2011)

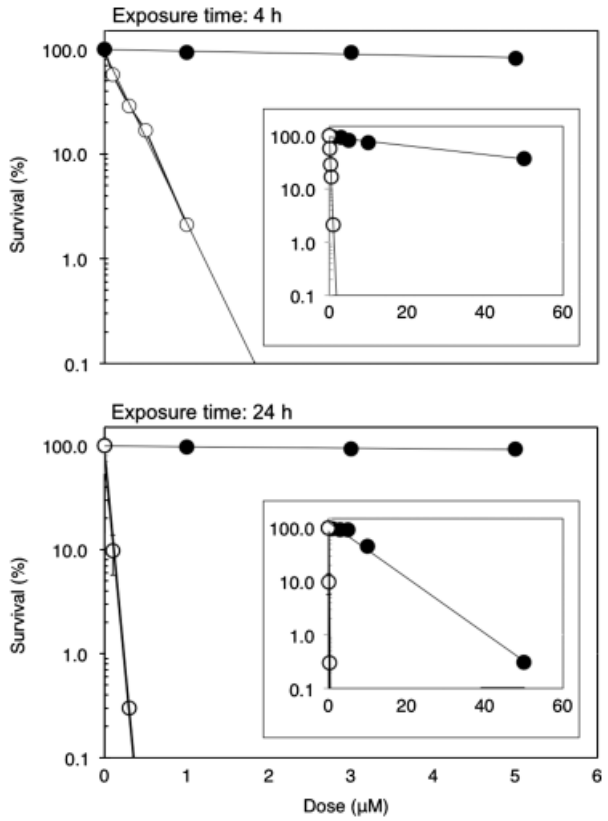

Fig. 2. The effects of AFB1 (closed circles) or Adriamycin (open circles) treatment of HepG2 cells for 4 h (top) or 24 h (bottom) on cell survival colony-forming ability. Cell survival was calculated as the per cent ratio of cell numbers in treated vs untreated cells ($n = 3$). Survival parameters were determined by plotting survival data on a semi-log plot. Insets: cell survival at higher AFB1 (up to 50 μmol/l) and Adriamycin (up to 5 μmol/l) doses. Error bars: SD. cell survival was determined by assessing cell growth in 100 mm dishes after exposure to AFB1 or Adriamycin. HepG2 cells were seeded in six-well plates and semiconfluent cells were exposed to AFB1 (0, 1, 3, 5, 10 and 50 μmol/l) or Adriamycin (0, 0.1, 0.3, 0.5, 1 and 5 μmol/l) for 4 or 24 h. Following exposure, 10^4 cells were seeded into 100-mm dishes and colonies were counted 10 days later. AFB1, aflatoxin B1; SD, standard deviation.

assays. Cell survival was determined by assessing colony growth in 100 mm dishes after exposure to AFB1 or Adriamycin. HepG2 cells were seeded in six-well plates and semiconfluent cells were exposed to AFB1 (0–50 μmol/l) in the presence of the S9-activation system. Control cells were treated with Adriamycin (0–5 μmol/l). Following 4 and 24 h of exposure, 10^4 cells were seeded into 100-mm dishes and colonies were counted 10 days later. Cell survival was calculated as the percent ratio of cell numbers in treated vs untreated cells. Survival parameters were determined by plotting survival data on a semi-log plot. AFB1 did not affect colony survival after 4 or 24 h of treatment at doses ≤ 5 μmol/l (Fig. 2, closed circles). In contrast, Adriamycin displayed a strong inhibition of colony survival, even with 50 times less concentrated molar doses (Fig. 2, open circles). Detectable effects of AFB1 were observed only when cells were exposed for 24 h at doses reaching 50 μmol/l (Fig. 2, bottom, inset).

We noticed that both AFB1 and Adriamycin displayed genotoxic effects that caused DNA breaks at comparable intensities (Fig. 1), but their effects on cell survival were highly different (Fig. 2). DNA damage usually triggers a strong cytotoxic response as observed here with Adriamycin (Fig. 2, open circles). This was not the case for AFB1-induced DNA damage that resulted in only a weak colony-inhibitory effect (Fig. 2, closed circles). In confirmation of these observations, 3 days of exposure to AFB1 did not induce a senescence response as tested by a senescence-associated β-galactosidase assay (Fig. S2A) nor apoptosis as tested by an activated caspase-3 assay (Fig. S2B). These findings prompted us to further explore the DNA damage response of HepG2 cells to AFB1.

DNA damage checkpoint foci induction by aflatoxin B1

To test the checkpoint response, we first used 53BP1 and phospho-H2AX foci assays (15) by immunofluorescence. Both AFB1 and Adriamycin induced 53BP1 and phospho-H2AX foci that were detectable after 3 days of culture, but AFB1-induced foci formation appeared to be less strong (Fig. 3). These findings provided evidence for a double-strand DNA break response (15, 16) to both agents, although the response appeared to be slightly different. We tested the statistical significance of AFB1-induced foci formation by counting cells with 53BP1-positive foci (> 5 foci/cell). Cells exposed to AFB1 between 1 and 72 h showed a progressive and statistically significant ($P < 0.0001$) accumulation of 53BP1 foci (Fig. S3). To test the duration of 53BP1 foci following a fixed time of exposure to AFB1, cells were first treated with AFB1 for 24 h and then cultivated in the absence of chemical treatment for up to 120 h. Cells with positive 53BP1 foci were detected by an indirect immunofluorescence assay (Fig. S4A) and then counted. As shown in Fig. S4B, the accumulation of 53BP1 foci peaked at 48 h of post-treatment, with 40% positive cells. A residual foci activity with 15–20% positive cells was detectable for at least 120 h in cells no longer exposed to AFB1. In contrast, cells exposed to DMSO only displayed low foci activity ($< 5\%$) throughout the experiment, indicating that increased foci formation was because of AFB1 exposure. Western blot analysis of the total 53BP1 protein demonstrated its higher expression in cells exposed to AFB1 for at least 72 h (Fig. S4C). Taken together, our findings indicated that following exposure to AFB1, HepG2 cells develop persistent 53BP1 foci that are compatible with a double-strand DNA break response lasting for several days.

Effects of aflatoxin B1 on HepG2 cell cycle progression

Based on observations indicating a defective growth response to AFB1 (Fig. 2), despite the formation of

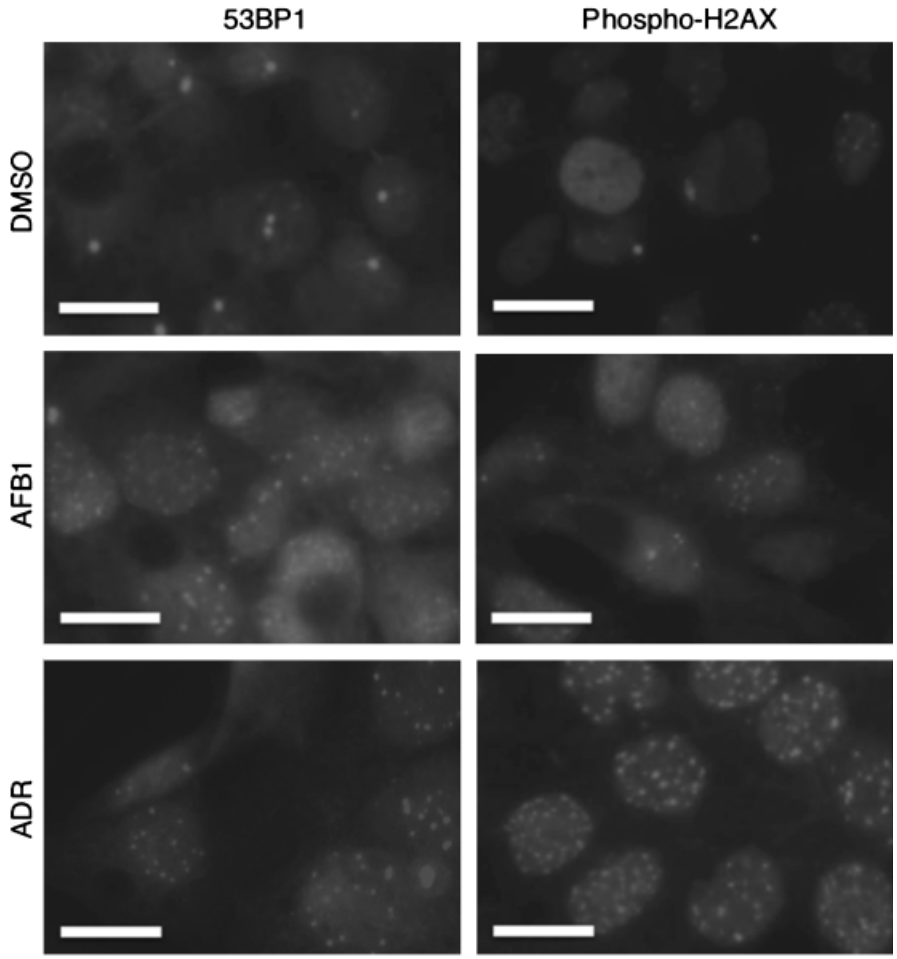

Fig. 3. Induction of 53BP1 and phospho-H2AX foci following AFB1 exposure in HepG2. Cells were treated with AFB1 (3 μmol/l) for 3 days and then subjected to 53BP1 and phoshpo-H2AX foci detection by indirect immunofluorescence. Control cells were exposed to DMSO only. Adriamycin (0.1 μmol/l) was used as a positive control. Scale bar = 20 μm. ADR, Adriamycin; AFB1, aflatoxin B1; DMSO, dimethyl sulphoxide.

persistent AFB1-DNA adducts (Fig. S1), DNA strand breaks (Fig. 1) and DNA damage foci (Figs. 3, S3 and S4), we performed time-course studies on cell cycle progression of HepG2 cells following AFB1 exposure. As shown in Figure 4, AFB1 exposure resulted in a transient accumulation of cells at the S phase (up to 26% from 13%, one-fold increase) at 24 h, followed by a return to control levels at 48 and 72 h. These changes were accompanied by a slight increase (40%) in G2/M-phase cells at 48 and 72 h, together with a slight decrease (18–26%) in G1-phase cells. These observations provided evidence for a transient and weak growth inhibition in HepG2 cells following AFB1 exposure (Fig. 4). The lack of a total cell cycle block under AFB1 exposure was compatible with a nearly complete colony survival after 5 μmol/l AFB1 exposure (Fig. 2). Of particular interest, AFB1-exposed HepG2 cells did not undergo G1 arrest despite the expression of wild-type p53, strongly suggesting that AFB1-induced DNA damage did not trigger a p53-dependent DNA damage response in these cells.

Incomplete DNA damage checkpoint response to aflatoxin B1 in different cell types

p53-dependent response to DNA damage is a strong mechanism protecting cells against the accumulation of deleterious mutations (15, 17, 30). Based on the current model for p53 activation upon DNA damage (15), we tested the status of critical components of DNA damage signalling after AFB1 exposure. Adriamycin and hydroxyurea were used for control experiments. As shown in Figure 5, Adriamycin treatment induced a typical double-strand break response in HepG2 cells by induced phosphorylations of H2AX, Chk2 and p53ser15, together with a weak induction of p53ser20 phosphorylation. Hydroxyurea treatment resulted in a weak phosphorylation of Chk1. As expected, we noted time-dependent differences in these responses. The response to AFB1 was globally weak or even absent. The only detectable response was observed with H2AX phosphorylation that was detectable after 24 h of AFB1 exposure, as well as

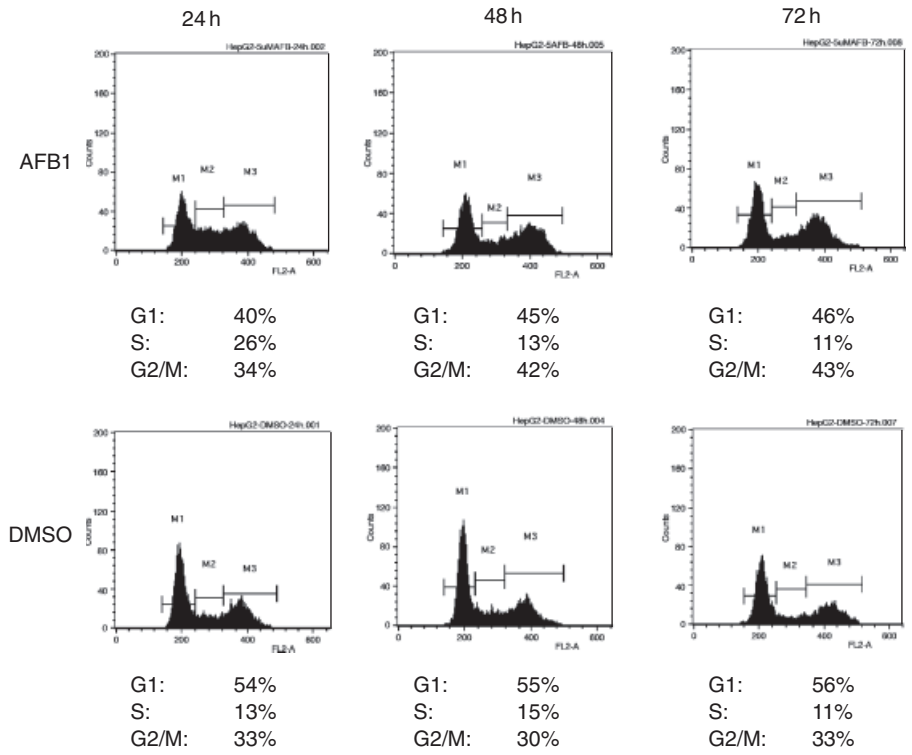

Fig. 4. The effects of AFB1 on HepG2 cell cycle distribution. Cells were treated with either 5 μmol/l AFB1 or DMSO up to 72 h, and cell cycle distribution was analysed by flow cytometry at 24, 48 and 72 h. AFB1, aflatoxin B1; DMSO, dimethyl sulphoxide.

after 24 h post-exposure. We performed additional studies with Huh7, an HCC cell line with retained activities for AFB1 activation (31), but displaying a homozygous p53 mutation (28). As shown in Fig. S5, Huh7 cells responded to Adriamycin by upregulation of phospho-H2AX levels only, and there was no phospho-Chk1 phosphorylation in response to hydroxyurea treatment. AFB1 did no affect phosphorylations of Chk1, chk2 or p53ser15, and the effect on H2AX phosphorylation was weakly detectable at 24 h of exposure. Taken together, these studies indicated that, apart from H2AX phosphorylation, critical components of DNA damage checkpoint proteins were not affected in hepatoma cells. In addition, the induction of p53 phosphorylation in response to DNA damage by Adriamycin appeared to be dependent on the wild type of the mutant status of p53 gene (see Fig. 5 in comparison with Fig. S5).

In order to further investigate the role of AFB1 in DNA damage response induction, we decided to explore wild-type p53-expressing HCT116 colorectal cancer cells and their p53 knockout HCT116–p53$^{-/-}$ derivatives (17). We performed all AFB1 experiments in these cell lines in the presence of the S9-activating system to allow the transformation of AFB1 into epoxy-AFB1 (32). First, we assessed the formation of DNA lesions following exposure to AFB1 (5 μmol/l) and Adriamycin (1 μmol/l). The response of HCT116 cells to both AFB1 and Adriamycin treatment was not different from the observations obtained with HepG2 cells. The great majority of cells stained positive for 8-hydroxydeoxyguanosine lesions following drug exposure (Fig. S6A) and displayed DNA double-strand breaks as tested by a neutral comet assay (Fig. S6B). Furthermore, HCT116 cells exposed to 5 μmol/l AFB1 for 24 h displayed a statistically significant ($P < 0.0001$) increase in both 53BP1 and phospho-H2AX-positive foci that lasted at least 48 h post-exposure, independent of *TP53* status (Fig. S7). Western blot analysis of critical components of DNA damage checkpoint response also provided results quite similar to that of HepG2. As shown in Fig. S8 and in comparison with Adriamycin and hydroxyurea, AFB1 treatment induced only a weak upregulation of phospho-H2AX levels at 24 h of exposure, with a more pronounced increase at 24 h of post-exposure.

Taken together, our observations with three different cell lines indicated that AFB1 induced a weak and delayed accumulation of phospho-H2AX. The phosphorylation of H2AX strongly suggested that AFB1-induced DNA damage triggered ATM activation by double-strand DNA breaks (15, 33). However, this ATM response was not accompanied by phosphorylations of Chk1, Chk2 or p53, three key proteins involved in the DNA damage checkpoint response. The lack of Chk1 phosphorylation after AFB1 exposure also suggested that the ATR/Chk1 pathway response was also inactive against AFB1-induced DNA damage.

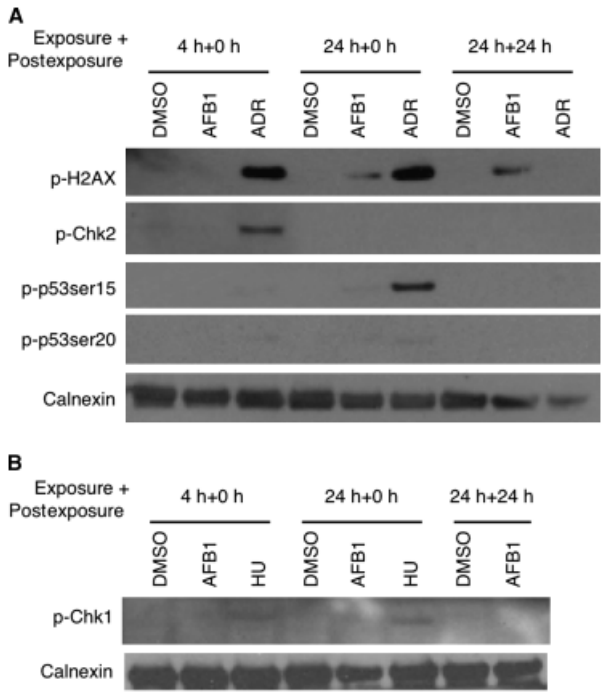

Fig. 5. Incomplete DNA damage checkpoint response of HepG2 cells to aflatoxin B1 (AFB1). HepG2 cells were treated with dimethyl sulphoxide (DMSO) or AFB1 (5 μmol/l) for 4 and 24 h, and tested immediately (4+0 h and 24+0 h) or after 24 h of incubation without treatment (24+24 h). HepG2 cells treated with 0.5 μmol/l Adriamycin (ADR) or 5 mmol/l hydroxyurea (HU) were used as positive controls for experiments shown in (A) and (B) respectively. Total cell lysates were subjected to western blot analysis. Calnexin was used as a loading control. p-H2AX, phospho-H2AX; p-p53ser15, phospho-p53ser15; p-p53ser20, phospho-p53ser20; p-Chk2, phospho-Chk2; p-Chk1, phospho-Chk1.

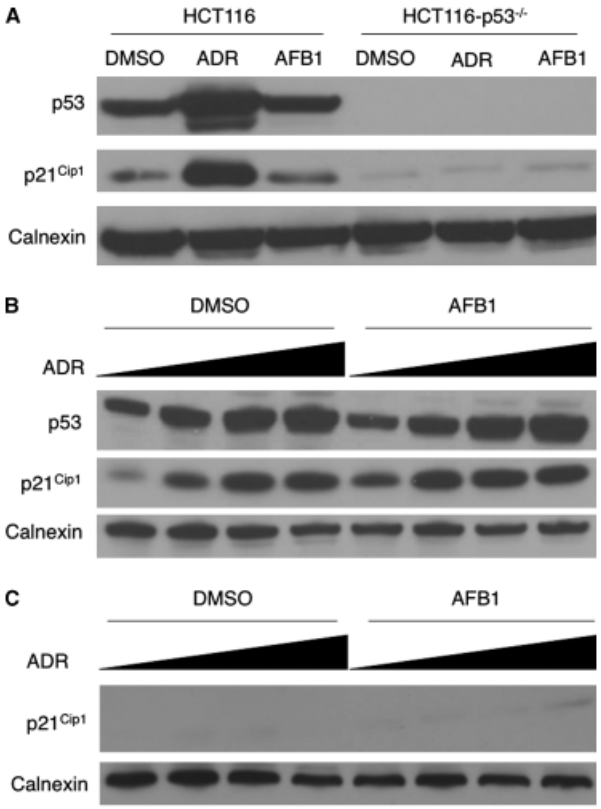

Fig. 6. Comparative analysis of the wild-type p53 response of HCT116 cells to AFB1 and Adriamycin treatment indicates that AFB1 cannot induce effective p53 activation. (A) Wild-type 53 HCT116 and p53-deficient HCT116-p53$^{-/-}$ cells were treated with AFB1 (3 μmol/l) or DMSO (in the presence of the S9-activating system) or Adriamycin (ADR; 1 μmol/l) for 24 h, followed by an additional cell culture in the absence of this chemical for another 24 h. (B and C) HCT116 (B) and HCT116-p53$^{-/-}$ (C) cells were cotreated with Adriamycin (ADR, increasing doses: 0, 0.1, 0.5 and 1 μmol/l respectively) in the absence (DMSO) or in the presence of 3 μmol/l AFB1, as described in (A) for 24 h (24 h pre-exposure to AFB1, followed by 24 h of co-exposure). Total cell lysates were used for western blot using anti-p53 and anti-p21^{Cip1} antibodies. Calnexin was used as a loading control. AFB1, aflatoxin B1; DMSO, dimethyl sulphoxide.

The mechanism of the inefficient DNA damage response to aflatoxin B1

As we observed similar responses of HCT116 and hepatoma cells to both AFB1 and Adriamycin treatment, we decided to further explore AFB1 effects using the isogenic HCT116 model, allowing us to better define its potential implications in p53-mediated DNA damage response. Before testing of AFB1 effects, we first examined the cell cycle responses of HCT116 and HCT116–p53$^{-/-}$ cells to Adriamycin. HCT116 cells displayed G1 and G2/M arrests in response to Adriamycin, associated with low levels of apoptosis (subG1 peak) and polyploidy formation at higher doses (Fig. S9A). There was also a depletion of S-phase cells as an indication of DNA synthesis inhibition that lasted at least 48 h following the removal of Adriamycin from the cell culture medium. The response of HCT116–p53$^{-/-}$ cells to Adriamycin was essentially similar, with the noticeable absence of a G1 peak (Fig. S9A). Based on Fig. S9B, which compares Adriamycin-induced cell cycle changes in wild-type and p53 knockout HCT116 cells, we concluded that DNA damage induced by Adriamycin is associated with a p53-dependent G1 arrest and a p53-independent G2/M arrest.

Our cell cycle studies with AFB1 treatment in the same cell lines are shown in Fig. S10. Unlike HepG2 cells, the HCT116 cell lines did not display a significant increase in S-phase cells. However, they displayed a weak decrease in the G1 phase, in parallel to a weak increase in G2/M cells, as observed with HepG2 cells. The response of HCT116–p53$^{-/-}$ cells to AFB1 exposure was not remarkable either, except for a slight increase in G2/M cells.

Taken together, these observations strongly suggested that human cells exposed to AFB1 could not develop a growth control response. The most likely reason for this was a delayed and deficient checkpoint response, including a lack of efficient phosphorylation of p53 protein. Therefore, we also compared the effects of AFB1 and Adriamycin on p53 and p21^{Cip1}. As shown in Figure 6A,

both p53 and $p21^{Cip1}$ responded to Adriamycin treatment with a dose-dependent increase in HCT116 cells. The increase in $p21^{Cip1}$ levels was p53-dependent, because we did not observe $p21^{Cip1}$ response in HCT116–$p53^{-/-}$ cells. In contrast, AFB1 treatment did not produce any detectable change in p53 levels in HCT116 cells. As a result, there was no detectable increase in $p21^{Cip1}$ in both HCT116 and HCT116–$p53^{-/-}$ cells. These findings suggested that either the AFB1 was actively involved in the inhibition of an effective DNA damage checkpoint response or the damage inflicted by AFB1 did not reach a threshold that is necessary for checkpoint activation, similar to previous observations with low-dose ionizing radiation (16). To test whether AFB1 inhibits the checkpoint response, we cotreated HCT116 cells with increasing doses of Adriamycin (0, 0.1, 0.5 and 1 μmol/l respectively) in the absence or presence of 3 μmol/l AFB1. As shown in Figure 6B and C, the accumulation of p53 and $p21^{Cip1}$ after Adriamycin exposure was not inhibited by AFB1 in HCT116 cells. Indeed, there was a slight increase in the accumulation $p21^{Cip1}$ after 0.1 μmol/l Adriamycin treatment in the presence of AFB1. The $p21^{Cip1}$ response of HCT116–$p53^{-/-}$ cells to Adriamycin was not affected by AFB1, except for a weak accumulation that was observed when cells were cotreated with 1 μmol/l Adriamycin and 3 μmol/l AFB1. These findings showed that AFB1 did not inhibit DNA damage checkpoint response under the conditions tested. Instead, AFB1 slightly stimulated the checkpoint response to Adriamycin.

Discussion

Hepatocellular cancer risk from aflatoxins, as well as aflatoxins' hepatocellular biochemistry, DNA interacting forms, the types of DNA damage and their repair by nucleotide excision, and their *in vitro* and *in vivo* mutagenic specificity for G → T transversions are well-established facts (34). Here, we addressed a less well-understood, but critical component of aflatoxin genotoxicity, namely the DNA damage checkpoint response. The *in vitro* experimental model system used here was designed after carefully considering previously described features associated with aflatoxin-related carcinogenicity. Human cells with a wild-type p53 expression were preferred because of the fact that a specific hotspot mutation of this gene was observed only in human HCC, not in other aflatoxin-induced mammalian tumours (35). We considered estimated chronic aflatoxin exposure levels in humans (0.01–0.3 μg/kg/day) (3) and hepatocarcinogenic doses (0.015–1 ppm) in rats (36). We also considered that 30 min of exposure to 1.6 μmol/l AFB1 was sufficient to induce p53-249 G → T mutations in HepG2 cells (37) and 0.2–5 μmol/l doses induced reporter gene mutations in mouse fibroblasts (32). Thus, the AFB1 doses that we used here (3–5 μmol/l) were at the upper limits of *in vitro* mutagenic activity in mammalian cells and were estimably superior to carcinogenic doses in humans and rats. We performed our cell response studies over a period of several days so that we could determine both immediate and delayed effects.

Our findings demonstrate that AFB1, when tested under conditions comparable with mutagenic and carcinogenic exposure levels, creates DNA adducts, 8-hydroxy-deoxyguanosine lesions and persistent strand breaks, but it does not lead to a sustained cell cycle arrest and/or an apoptosis response. AFB1 adducts are repaired by nucleotide excision repair (8); however, their removal is slow (6) and they remain at maximum levels for several days and are detectable over several weeks in rat liver cells (6, 7). The unusual stability of AFB1 adducts together with a slow repair process could account for their strong genotoxic effects. The expansion of cells with unrepaired DNA lesions could cause mutations in their genomes. Therefore, such cells are under the strict control of DNA damage checkpoint proteins that block cell cycle and/or induce apoptosis (15, 16, 30). Our *in vitro* findings and previously reported *in vivo* studies strongly suggest that cells exposed to mutagenic doses of AFB1 cannot develop a strong cell cycle arrest and/or apoptosis response. Our detailed analysis of DNA damage checkpoint proteins provides a plausible explanation for the uncoupling between DNA damage and growth control following AFB1 exposure. AFB1-exposed cells displayed DNA damage foci formation with both 53BP1 and phospho-H2AX marker proteins. These findings suggest that AFB1-induced DNA damage might trigger a checkpoint response compatible with a double-strand break-type response involving ATM. However, this response was weak and delayed, as indicated by phospho-H2AX levels tested by western blot analysis. Our western blot studies for phospho-ATM levels after AFB1 exposure provided inconsistent results with or without an increase (data not shown), further indicating that ATM is not activated consistently following AFB1-induced DNA damage. In confirmation of this hypothesis, AFB1-induced DNA damage failed to activate Chk2 and p53ser15 phosphorylations. The alternative DNA damage checkpoint response mediated by ATR and Chk1 was also ineffective, as tested by Chk1 and p53ser20 phosphorylation. The most important outcome of a deficient response to AFB1 was a lack of cell growth control. Apart from a slight and transient increase in the G2/M phase, cells did not undergo stable cell cycle arrest, senescence and/or apoptosis. Consequently, the overall cell survival was not affected even after exposure to 5 μmol/l AFB1. It was necessary to expose cells to 50 μmol/l AFB1 for at least 24 h in order to observe a cytotoxic effect. Such a high dose represents a more than 150-fold higher value when compared with effective doses of Adriamycin in the same type of cells.

The mechanisms of the failing checkpoint response to AFB1 are currently unknown. We speculate that AFB1 is able to induce DNA damage, without triggering an effective damage response signal at doses $\leq$ 5 μmol/l. The delayed and defective DNA damage response to AFB1 could be related to the type of DNA and protein adducts that it forms in exposed cells (5, 8). AFB1 DNA adducts that are known to be repaired primarily by nucleotide excision

repair (8) may not be sufficient to trigger directly a strong DNA damage response, which usually requires single- and double-strand DNA breaks (15, 16). Instead, the DNA breaks could occur during the repair process causing a delayed response, as suggested by a weak and delayed occurrence of phospho-H2AX accumulation observed here. Alternatively, or in addition, adducts of AFB1 formed with critical cellular proteins may hamper an effective damage response. This alternative is highly unlikely, as suggested by the inability of AFB1 cotreatment to inhibit Adriamycin-induced accumulation of p53 and $p21^{Cip1}$ as an end-point reporter for checkpoint response. Thus, our findings favour the hypothesis that AFB1-induced DNA damage, tested here at doses $\leq 5\,\mu mol/l$, did not reach the threshold for an efficient induction of checkpoint response. At higher doses, AFB1 is probably effective to trigger a DNA damage response. Indeed, it has been reported previously that HepG2 cells exposed to 10 µmol/l AFB1 can elicit a cell cycle arrest response (38). When tested with 5 mg/kg dose, AFB1 exposure could induce $p21^{Cip1}$ upregulation in rat liver (39). However, as stressed earlier, cancer-causing dietary exposure to AFB1 occurs at low levels, a condition that is similar to our *in vitro* conditions that provided evidence for a defective checkpoint response.

A defective or a negligent G2/M checkpoint response to low ionizing radiation exposure has been postulated by Löbrich and Jeggo (16) as a potential cause of genomic instability and cancer risk. The authors also proposed that a master p53-dependent G1 checkpoint might remain effective during a negligent G2/M checkpoint for later elimination of escaping cells. Our findings strongly suggest that the DNA damage checkpoint in response to low doses of AFB1 is defective, negligent or delayed. In addition, a p53-dependent salvage pathway is apparently ineffective against AFB1-induced DNA damage. The lack of an efficient response to AFB1-induced DNA damage may be because of the type of lesion(s) induced at the DNA and/or protein levels by activated AFB1 in exposed cells. It will be interesting to further investigate these issues in future studies.

In conclusion, our findings provide *in vitro* evidence for a negligent G1 and G2/M checkpoint response to AFB1-induced DNA damage. This defective response may contribute to the mutagenic and carcinogenic potencies of aflatoxins.

Acknowledgements

O. G. Y. and H. Y. were supported by short-term European Molecular Biology Organization (EMBO), and O. G. Y., H. Y. and M. Y. by long-term The Scientific and Technological Research Council of Turkey (TUBITAK) PhD fellowships respectively. We would like to thank Stefan Dimitrov for his critical reading of the manuscript and helpful suggestions.

Funding: this work was supported by grants from the Institut National de Cancer (France), The Scientific and Technological Research Council of Turkey (TUBITAK) and State Planning Office of Turkey (DPT). Additional support was provided by the Turkish Academy of Sciences. The funders had no role in the study design, data collection and analysis, decision to publish or preparation of the manuscript.

Conflict of interest statement: none declared.

References

1. Parkin DM. The global health burden of infection-associated cancers in the year 2002. *Int J Cancer* 2006; **118**: 3030–44.
2. Wild CP, Montesano R. A model of interaction: aflatoxins and hepatitis viruses in liver cancer aetiology and prevention. *Cancer Lett* 2009; **286**: 22–8.
3. Liu Y, Wu F. Global burden of aflatoxin-induced hepatocellular carcinoma: a risk assessment. *Environ Health Perspect* 2010; **118**: 818–24.
4. Wang JS, Groopman JD. DNA damage by mycotoxins. *Mutat Res* 1999; **424**: 167–81.
5. Wild CP, Gong YY. Mycotoxins and human disease: a largely ignored global health issue. *Carcinogenesis* 2010; **31**: 71–82.
6. Croy RG, Wogan GN. Temporal patterns of covalent DNA adducts in rat liver after single and multiple doses of aflatoxin B1. *Cancer Res* 1981; **41**: 197–203.
7. Smela ME, Hamm ML, Henderson PT, *et al.* The aflatoxin B(1) formamidopyrimidine adduct plays a major role in causing the types of mutations observed in human hepatocellular carcinoma. *Proc Natl Acad Sci USA* 2002; **99**: 6655–60.
8. Bedard LL, Massey TE. Aflatoxin B1-induced DNA damage and its repair. *Cancer Lett* 2006; **241**: 174–83.
9. Shen HM, Ong CN, Lee BL, Shi CY. Aflatoxin B1-induced 8-hydroxydeoxyguanosine formation in rat hepatic DNA. *Carcinogenesis* 1995; **16**: 419–22.
10. Bressac B, Kew M, Wands J, Ozturk M. Selective G to T mutations of p53 gene in hepatocellular carcinoma from southern Africa. *Nature* 1991; **350**: 429–31.
11. Ozturk M. P53 mutation in hepatocellular carcinoma after aflatoxin exposure. *Lancet* 1991; **338**: 1356–9.
12. Hsu IC, Metcalf RA, Sun T, *et al.* Mutational hotspot in the p53 gene in human hepatocellular carcinomas. *Nature* 1991; **350**: 427–8.
13. Aguilar F, Harris CC, Sun T, Hollstein M, Cerutti P. Geographic variation of p53 mutational profile in nonmalignant human liver. *Science* 1994; **264**: 1317–9.
14. Kirk GD, Lesi OA, Mendy M, *et al.* 249(ser) TP53 mutation in plasma DNA, hepatitis B viral infection, and risk of hepatocellular carcinoma. *Oncogene* 2005; **24**: 5858–67.
15. Sancar A, Lindsey-Boltz LA, Unsal-Kacmaz K, Linn S. Molecular mechanisms of mammalian DNA repair and the DNA damage checkpoints. *Annu Rev Biochem* 2004; **73**: 39–85.
16. Löbrich M, Jeggo PA. The impact of a negligent G2/M checkpoint on genomic instability and cancer induction. *Nat Rev Cancer* 2007; **7**: 861–9.
17. Bunz F, Dutriaux A, Lengauer C, *et al.* Requirement for p53 and p21 to sustain G2 arrest after DNA damage. *Science* 1998; **282**: 1497–501.

18. Dreiem A, Fonnum F. Thiophene is toxic to cerebellar granule cells in culture after bioactivation by rat liver enzymes. *Neurotoxicology* 2004; **25**: 959–66.
19. Erexson GL, Periago MV, Spicer CS. Differential sensitivity of Chinese hamster V79 and Chinese hamster ovary (CHO) cells in the in vitro micronucleus screening assay. *Mutat Res* 2001; **495**: 75–80.
20. Yarborough A, Zhang YJ, Hsu TM, Santella RM. Immunoperoxidase detection of 8-hydroxydeoxyguanosine in aflatoxin B1-treated rat liver and human oral mucosal cells. *Cancer Res* 1996; **56**: 683–8.
21. Hsieh LL, Hsu SW, Chen DS, Santella RM. Immunological detection of aflatoxin B1-DNA adducts formed in vivo. *Cancer Res* 1988; **48**: 6328–31.
22. Ozturk N, Erdal E, Mumcuoglu M, *et al.* Reprogramming of replicative senescence in hepatocellular carcinoma-derived cells. *Proc Natl Acad Sci USA* 2006; **103**: 2178–83.
23. Olive PL, Durand RE, Le Riche J, Olivotto IA, Jackson SM. Gel electrophoresis of individual cells to quantify hypoxic fraction in human breast cancers. *Cancer Res* 1993; **53**: 733–6.
24. Olive PL, Banath JP. Detection of DNA double-strand breaks through the cell cycle after exposure to X-rays, bleomycin, etoposide and 125IdUrd. *Int J Radiat Biol* 1993; **64**: 349–58.
25. Chandna S. Single-cell gel electrophoresis assay monitors precise kinetics of DNA fragmentation induced during programmed cell death. *Cytometry A* 2004; **61**: 127–33.
26. Senturk S, Mumcuoglu M, Gursoy-Yuzugullu O, *et al.* Transforming growth factor-beta induces senescence in hepatocellular carcinoma cells and inhibits tumor growth. *Hepatology* 2010; **52**: 966–74.
27. Knasmuller S, Parzefall W, Sanyal R, *et al.* Use of metabolically competent human hepatoma cells for the detection of mutagens and antimutagens. *Mutat Res* 1998; **402**: 185–202.
28. Puisieux A, Ji J, Guillot C, *et al.* P53-mediated cellular response to DNA damage in cells with replicative hepatitis B virus. *Proc Natl Acad Sci USA* 1995; **92**: 1342–6.
29. Puisieux A, Galvin K, Troalen F, *et al.* Retinoblastoma and p53 tumor suppressor genes in human hepatoma cell lines. *FASEB J* 1993; **7**: 1407–13.
30. Meek D W. Tumour suppression by p53: a role for the DNA damage response? *Nat Rev Cancer* 2009; **9**: 714–23.
31. Sivertsson L, Ek M, Darnell M, *et al.* CYP3A4 catalytic activity is induced in confluent Huh7 hepatoma cells. *Drug Metab Dispos* 2010; **38**: 995–1002.
32. Besaratinia A, Kim SI, Hainaut P, Pfeifer GP. In vitro recapitulating of TP53 mutagenesis in hepatocellular carcinoma associated with dietary aflatoxin B1 exposure. *Gastroenterology* 2009; **137**: 1127–37, 37 e1–5.
33. Burma S, Chen BP, Murphy M, Kurimasa A, Chen DJ. ATM phosphorylates histone H2AX in response to DNA double-strand breaks. *J Biol Chem* 2001; **276**: 42462–7.
34. Groopman JD, Kensler TW, Wild CP. Protective interventions to prevent aflatoxin-induced carcinogenesis in developing countries. *Annu Rev Public Health* 2008; **29**: 187–203.
35. Gouas D, Shi H, Hainaut P. The aflatoxin-induced TP53 mutation at codon 249 (R249S): biomarker of exposure, early detection and target for therapy. *Cancer Lett* 2009; **286**: 29–37.
36. Newberne PM, Wogan GN. Sequential morphologic changes in aflatoxin B carcinogenesis in the rat. *Cancer Res* 1968; **28**: 770–81.
37. Aguilar F, Hussain SP, Cerutti P. Aflatoxin B1 induces the transversion of G → T in codon 249 of the p53 tumor suppressor gene in human hepatocytes. *Proc Natl Acad Sci USA* 1993; **90**: 8586–90.
38. Ricordy R, Gensabella G, Cacci E, Augusti-Tocco G. Impairment of cell cycle progression by aflatoxin B1 in human cell lines. *Mutagenesis* 2002; **17**: 241–9.
39. Ellinger-Ziegelbauer H, Stuart B, Wahle B, Bomann W, Ahr HJ. Characteristic expression profiles induced by genotoxic carcinogens in rat liver. *Toxicol Sci* 2004; **77**: 19–34.

Supporting information

Additional supporting information may be found in the online version of this article:

Figure S1. Induction of DNA adducts and 8-hydroxy-deoxyguanosine lesions following AFB1 exposure in HepG2.

Figure S2. Induction of senescence arrest and apoptosis in HepG2 cells by Adriamycin, but not AFB1 in HepG2.

Figure S3. Time-dependent increase in 53BP1 foci-positive HepG2 cells under AFB1 exposure.

Figure S4. The duration of 53BP1 foci after 24 h of exposure to AFB1 in HepG2.

Figure S5. Incomplete DNA damage checkpoint response of Huh7 hepatoma cells to AFB1.

Figure S6. Induction of 8-hydroxy-deoxyguanosine lesions and double-strand breaks in HCT116 isogenic clones following AFB1 exposure.

Figure S7. Increased DNA damage-induced foci detection after exposure of HCT116 isogenic clones to AFB1.

Figure S8. Incomplete DNA damage checkpoint response of wild-type p53 HCT116 cells to AFB1.

Figure S9. p53-dependent and p53-independent cell cycle arrest in HCT116 isogenic clones after Adriamycin treatment.

Figure S10. Lack of cell cycle arrest of HCT116 isogenic clones in response to AFB1-induced DNA damage.

Please note: Wiley-Blackwell is not responsible for the content or functionality of any supporting materials supplied by the authors. Any queries (other than missing material) should be directed to the corresponding author for the article.